The EMBO Journal (2005) 24, 11–22 | © 2005 European Molecular Biology Organization | All Rights Reserved 0261-4189/05
www.embojournal.org

THE EMBO JOURNAL

Selenocysteine tRNA-specific elongation factor SelB is a structural chimaera of elongation and initiation factors

Marc Leibundgut[1], Christian Frick[1], Martin Thanbichler[2], August Böck[2] and Nenad Ban[1,*]

[1]Institut für Molekularbiologie und Biophysik, Eidgenössische Technische Hochschule Zürich, Zürich, Switzerland and [2]Departement Biologie I der Universität München, München, Germany

In all three kingdoms of life, SelB is a specialized translation elongation factor responsible for the cotranslational incorporation of selenocysteine into proteins by recoding of a UGA stop codon in the presence of a downstream mRNA hairpin loop. Here, we present the X-ray structures of SelB from the archaeon *Methanococcus maripaludis* in the apo-, GDP- and GppNHp-bound form and use mutational analysis to investigate the role of individual amino acids in its aminoacyl-binding pocket. All three SelB structures reveal an EF-Tu:GTP-like domain arrangement. Upon binding of the GTP analogue GppNHp, a conformational change of the Switch 2 region in the GTPase domain leads to the exposure of SelB residues involved in clamping the 5′ phosphate of the tRNA. A conserved extended loop in domain III of SelB may be responsible for specific interactions with tRNA^{Sec} and act as a ruler for measuring the extra long acceptor arm. Domain IV of SelB adopts a β barrel fold and is flexibly tethered to domain III. The overall domain arrangement of SelB resembles a 'chalice' observed so far only for initiation factor IF2/eIF5B. In our model of SelB bound to the ribosome, domain IV points towards the 3′ mRNA entrance cleft ready to interact with the downstream secondary structure element.

The EMBO Journal (2005) **24,** 11–22. doi:10.1038/sj.emboj.7600505; Published online 23 December 2004
Subject Categories: structural biology; RNA
Keywords: initiation; protein synthesis; pyrrolysine; SECIS; selenocysteine

Introduction

Selenium is a trace element that is incorporated into proteins in the form of selenocysteine (Sec) in all three kingdoms (Kyriakopoulos and Behne, 2002). It is found mainly in the active site of oxidoreductases, where it is directly involved in catalysis. Unlike cysteine (Cys), Sec is negatively charged at physiological pH and highly reactive. In mammals, Sec is essential for viability, is present in enzymes involved in detoxifying reactive oxygen species and hormone biosynthesis and plays a key role in fundamental biological processes like development, reproduction, immune function, ageing, cancer, viral infections and cardiovascular disorders (Hatfield, 2001).

Sec is incorporated into proteins during translation elongation and is encoded by a combination of an internal UGA stop codon and a specific mRNA hairpin structure located further downstream, the SECIS (selenocysteine inserting sequence) element (Baron and Böck, 1995; Atkins and Gesteland, 2000). Both Sec determinants have to be recognized for reading through the stop codon instead of terminating translation. The specificity for the stop codon is achieved by tRNA^{Sec}, whose UCA anticodon is complementary to the UGA stop codon. The specialized translation elongation factor SelB binds Sec-tRNA^{Sec} in a GTP-dependent manner. This is in analogy to EF-Tu, which shares sequence homology with SelB for domains I, II and III (Hilgenfeld *et al*, 1996). However, SelB delivers Sec-tRNA^{Sec} to the ribosomal A site only in the presence of the *cis*-acting SECIS element.

In bacteria, SelB binds the SECIS element, located immediately downstream of the internal UGA stop codon, directly via a C-terminal, 24 kDa extension (domain IV), which is absent in EF-Tu (Zinoni *et al*, 1990; Kromayer *et al*, 1996; Fourmy *et al*, 2002; Selmer and Su, 2002). In mammals, SelB domain IV is considerably shorter and binds to SBP2 (SECIS binding protein 2), a 94 kDa adapter protein, which recognizes the SECIS element and forms a quarternary complex together with SelB:Sec-tRNA^{Sec}:GTP (Copeland *et al*, 2000; Tujebajeva *et al*, 2000; Zavacki *et al*, 2003). Mammalian SECIS elements are found in the 3′ untranslated region (UTR) of the mRNA and can recode several internal UGA stop codons per gene (Berry *et al*, 1991; Hill *et al*, 1993).

The discovery of archaeal SelB homologues in *Methanococcus jannaschii* and *Methanococcus maripaludis* revealed an elongation factor with an even shorter, 8 kDa C-terminal extension (Rother *et al*, 2000, 2003). This, together with the finding of a gene harbouring two internal stop codons and only one SECIS element in the 3′ UTR, led to the proposal of a mechanism similar to the mammalian, adapter-mediated system (Rother *et al*, 2001). However, an SBP2 homologue has not been discovered in archea so far.

SelB specifically recognizes selenocysteylated tRNA^{Sec} but not other tRNAs, whereas EF-Tu binds all elongator tRNAs except tRNA^{Sec} (Forchhammer *et al*, 1989; Förster *et al*, 1990; Fagegaltier *et al*, 2000; Rother *et al*, 2000). Compared to canonical tRNAs, key differences in the secondary structure of tRNA^{Sec} may serve as identity elements for this specificity. In archaeal and eukaryotic tRNA^{Sec}, the prolonged 9 bp acceptor stem together with the shortened 4 bp T stem is proposed to form a 13 bp acceptor arm (the 9/4 model), 1 bp longer than observed for canonical tRNAs, which adopt a 7/5 conformation (Hubert *et al*, 1998). In bacterial tRNA^{Sec}, the 13 bp acceptor arm is formed by an 8 bp acceptor stem and a

*Corresponding author. Institute for Molecular Biology and Biophyiscs, Swiss Federal Institute of Technology, ETH Hönggerberg, HPK Building, Zurich, Switzerland. Tel.: +41 1 633 2785; Fax: +41 1 633 1246; E-mail: ban@mol.biol.ethz.ch

Received: 5 October 2004; accepted: 12 November 2004; published online: 23 December 2004

5 bp T stem (the 8/5 model; Baron *et al*, 1993). The identity of $tRNA^{Sec}$ is likely determined by the unusual length of the acceptor arm helix (Baron and Böck, 1991). Interestingly, eukaryotic $tRNA^{Sec}$ is bound by *Escherichia coli* SelB *in vitro* and complements for the endogenous $tRNA^{Sec}$ *in vivo*, indicating the conservation of structural features among kingdoms that are important for $tRNA^{Sec}$ recognition by SelB (Baron *et al*, 1994).

In an unusual biosynthetic pathway, $tRNA^{Sec}$ is initially charged with serine (Ser) by SerRS, the common aminoacyl-tRNA synthetase for all isoaccepting $tRNA^{Ser}$, to form Ser-$tRNA^{Sec}$ and is further converted enzymatically to Sec-$tRNA^{Sec}$ (Commans and Böck, 1999). In order to prevent misincorporation during translation, SelB:GTP specifically binds selenocysteylated $tRNA^{Sec}$, but neither the serylated nor the uncharged $tRNA^{Sec}$ precursors (Forchhammer *et al*, 1989; Fagegaltier *et al*, 2000; Rother *et al*, 2000).

In order to gain insights into the molecular mechanism of the recoding process during Sec incorporation, we have determined the X-ray structures of full-length SelB from *M. maripaludis* in the GDP-, GppNHp- and apo-form.

Results

Crystallization and structure determination

X-ray quality crystals were grown from full-length *M. maripaludis* SelB in complex with GDP (Materials and methods and Supplementary data). The crystals contained four molecules per asymmetric unit and the structure was solved using mercury SAD phasing (Table I).

Despite their high flexibility, it was possible to build the complete structure for one of the four molecules in the asymmetric unit (molecule C, residues 1–468). In the other three molecules (A, B and D), a few segments were excluded from the refinement due to weak electron density (Supplementary data). Therefore, the coordinates of molecule C were used for the structure analysis described here unless stated otherwise. SelB molecules A, B and C contain GDP in their nucleotide-binding pocket, whereas molecule D is in the nucleotide free form. Sulphate ions are observed at the GTP-γ phosphate position of molecules A and B, where they may mimic an intermediate state of SelB prior to the release of inorganic phosphate. However, they do not affect the GDP conformation of these SelB molecules.

For obtaining SelB-apo crystals, GDP was either omitted from the crystallization solution or removed by buffer exchange during the stabilization of GDP-grown crystals (Materials and methods and Supplementary data). Apart from the absence of GDP in the nucleotide-binding pocket, only minor structural differences were observed. Therefore, we conclude that the SelB-apo structure is very similar to the structure of the molecule in the GDP form and will not discuss it in further detail.

For SelB:GTP, mercury SAD data were collected from crystals containing either cocrystallized or soaked GppNHp, a nonhydrolysable GTP analogue (Materials and methods,

Table I Data collection, phasing and refinement statistics of SelB crystals

Crystal form	SelB:GDP	SelB:GppNHp	SelB-apo
Data collection			
Wavelength (Å)	0.9724	1.0000	1.0000
Space group	$P3_112$	$P3_112$	$P3_112$
Unit cell parameters	$a=b=146.8$ Å, $c=297.3$ Å	$a=b=146.7$ Å, $c=297.0$ Å	$a=b=146.8$ Å, $c=297.2$ Å
Mosaicity (deg)	0.35	0.53	0.59
Total reflections	1 261 483	1 009 218	1 074 795
Unique reflections	73 441	60 640	66 724
Resolution range (Å)	50–3.0	50–3.2	50–3.1
R_{sym} (%)[a]	11.7	15.4	13.1
Completeness (%)[b]	100 (99.8)	100 (100)	99.9 (99.9)
I/σ[b]	25.8 (1.7)	14.7 (1.5)	18.3 (2.7)
Phasing power[c]	1.187	0.747	0.913
Combined FOM[d]	0.210	0.135	0.161
Number of sites	16	16	16
Refinement[e]			
Resolution range (Å)	40–3.0	40–3.2	40–3.1
R, R_{free}[f] (%)	31.7, 32.9	34.7, 36.5	33.6, 34.7
Completeness (%)[b,g]	80.7 (58.4)	69.6 (41.1)	76.3 (65.1)
R.m.s.d. bonds (Å)	0.011	0.013	0.012
R.m.s.d. angles (deg)	1.7	1.8	1.7
Luzzati error (Å)[h]	0.59	0.62	0.58
Monomers/asymmetric unit	4	4	4
Number of protein residues	1649	1649	1650
Number of ligands	21	17	16
Solvent content (%)	71	71	71
$\langle B_{total} \rangle$ (Å^2)	90.7	93.9	73.2

[a]$R_{sym}=\sum|I_{obs}-\langle I\rangle|/\sum\langle I\rangle$.
[b]Values for highest resolution shells are given in parentheses.
[c]Phasing power (centric/acentric) = r.m.s. F_h/E_{iso}, where E_{iso} is the lack of closure error.
[d]FOM, figure of merit. FOM = $\langle \cos(\Delta\alpha_h)\rangle$, where $\Delta\alpha_h$ is the error in the phase angle for reflection h.
[e]For SelB:GDP refinement, data of three isomorphous crystals were combined.
[f]R_{free} based on 10% of the data excluded from refinement.
[g]Due to anisotropic diffraction, only reflections with $I/\sigma>2$ were used for refinement. Therefore, the overall and highest 0.1 Å resolution shell completeness during refinement is also indicated.
[h]Estimated Luzzati coordinate error (5.0 Å−high-resolution limit).

Supplementary data and Table I). GppNHp was present in molecules A and B, whereas molecules C and D are in the nucleotide free form. Interestingly, we detected a conformational change in the Switch 2 region of domain I in molecule A.

Overall structure and domain arrangement in SelB

SelB:GDP has overall dimensions of 110 Å × 66 Å × 39 Å and consists of four distinct structural domains (domains I–IV) that adopt a 'molecular chalice' arrangement (Figure 1A). The first three domains form the cup of the chalice, whereas its base is formed by domain IV, which is linked to the cup via two long, antiparallel β strands. Comparing molecules A and C in the crystal reveals the flexibility of the linker between domains III and IV (Figure 1B). After superposition of the first three domains with a root mean square deviation of the carbon α atoms ($rmsd_{C\alpha}$) of 1.7 Å, the orientation of domain IV differs by 20°. Interestingly, SelB domains I–III, consisting of EF-Tu related secondary structure elements, adopt an overall EF-Tu:GTP-like domain arrangement not only in the SelB:GppNHp but also in the SelB:GDP and SelB-apo forms (Berchtold *et al*, 1993; Kjeldgaard *et al*, 1993; Nissen *et al*, 1995, 1999). By superimposing SelB:GDP with EF-Tu:GppNHp, the $rmsd_{C\alpha}$ is only 2.6 Å for 288 corresponding residues. All four SelB molecules in the asymmetric unit, which are related by arbitrary noncrystallographic symmetry transformations, adopt the GTP-like conformation. This is in agreement with the results of our alkaline deacylation experiments, which show that *E. coli* SelB is able to bind Sec-$tRNA^{Sec}$ in the apo- and GDP form with lower than 100 nM affinity (data not shown). EF-Tu:GDP, in contrast, has a much lower affinity for aminoacylated tRNAs ($K_d = 29$ μM; Dell *et al*, 1990). The affinity of *E. coli* SelB:GDP for Sec-$tRNA^{Sec}$ is comparable to that of initiation factor IF2γ:GDP for Met-$tRNA_i^{Met}$ ($K_d = 140$ nM; Kapp and Lorsch, 2004). Strikingly, IF2γ is not only a close structural homologue of SelB for domains I–III, but also adopts a GTP-like overall domain arrangement in the apo- and GDP form ($rmsd_{C\alpha} = 3.2$ Å of SelB:GDP and IF2γ:GDP for 279 corresponding residues; Schmitt *et al*, 2002; Roll-Mecak *et al*, 2004). In addition, a GTP-like conformation of domain II relative to domain I has been observed in the apo- and GDP form of elongation factor EF-G (Ævarsson *et al*, 1994; Czworkowski *et al*, 1994) and initiation factor IF2/eIF5B (Roll-Mecak *et al*, 2000). Therefore, we believe that the GTP-like domain arrangement is not induced due to crystal packing in SelB. Interestingly, the overall shape of SelB strikingly resembles the shape of IF2/eIF5B, in spite of significant topological differences (Figure 6A; Roll-Mecak *et al*, 2000).

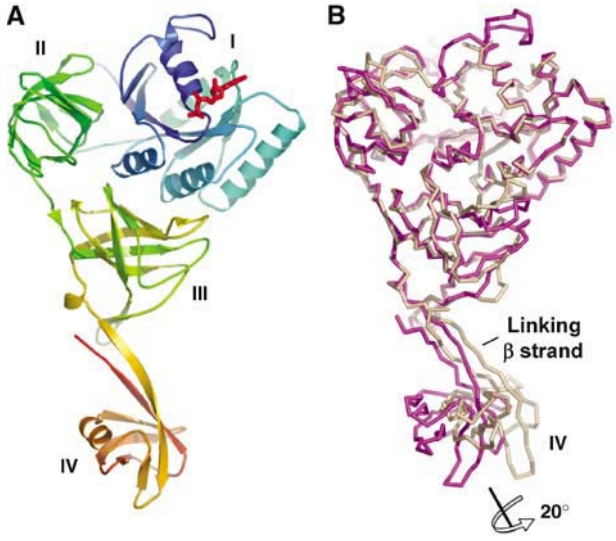

Figure 1 Overview of the SelB:GDP structure from *M. maripaludis*. (**A**) Structure of SelB molecule C in the GDP conformation. The Cα trace is rainbow coloured from the N- (blue) to the C-terminus (orange). SelB consists of four individual domains, denoted I, II, III and IV, which are arranged to form a 'molecular chalice'. The first three domains form the cup and the fourth the base of the chalice. The GDP nucleotide (red) is bound to domain I (blue), which carries the GTPase activity. (**B**) Flexibility of domain IV demonstrated by superposition of two different SelB:GDP molecules (chains A and C) in the asymmetric unit. The superposition of the first three domains shows that domain IV is flexibly linked to domain III. Its orientation in these two snapshots varies by an approximately 20° rotation.

Topology of individual domains

The basic topology of domain I (residues 1–175), which binds the nucleotide and carries the GTPase activity, consists of a six-stranded central β sheet surrounded by five α helices (Figures 1A and 2). Helices α2, α3 and α4 are on one side of the sheet, whereas α1 and α5 are on the other. Compared to domain I of *T. aquaticus* EF-Tu, the thermophile loop located between β6 and α5 is reduced to a short turn in SelB (Figure 2; Kjeldgaard *et al*, 1993; Nissen *et al*, 1999). Excluding this loop and the Switch 1 and 2 regions from the calculation, the $rmsd_{C\alpha}$ difference between the two factors is 1.7 Å for 130 corresponding residues. The comparison of SelB with the structures of IF2γ from *M. jannaschii* and *P. abyssi* (Schmitt *et al*, 2002; Roll-Mecak *et al*, 2004), which is the other factor that specifically recognizes a noncanonical tRNA (initiator $tRNA_i^{Met}$), reveals a high degree of structural homology to SelB domain I. The major difference is the zinc-binding motif of IF2γ, which is absent in SelB (Figure 2). By omitting the zinc knuckle from the calculation, the pairwise $rmsd_{C\alpha}$ of IF2γ:GDP and SelB:GDP is only 1.4 Å for 141 residues. These findings support the idea that IF2γ and SelB are evolutionarily closely related: A phylogenetic analysis of bacterial SelB and eukaryotic/archaeal IF2γ sequences performed by Keeling *et al* (1998) revealed that both factors are members of the same family but are different from the EF-Tu family.

SelB domain II (residues 186–268) adopts a β barrel topology consisting of 10 β strands, β7–β16 (Figures 1A and 2). In spite of the overall similarity with EF-Tu (pairwise $rmsd_{C\alpha} = 1.6$ Å for 79 residues), several residues directly involved in the recognition of the tRNA 3′ aminoacyl group in EF-Tu are different in SelB and therefore could play an important role in the specificity of Sec recognition.

Domain III of SelB (residues 274–378) is formed by strands β17–β27, which are arranged to form a β barrel (Figure 1A). At the sequence level, the similarity between SelB and EF-Tu domain III is low (Figure 2). However, the comparison of the structures reveals that they adopt the same fold (pairwise $rmsd_{C\alpha} = 1.4$ Å for 81 residues). Interestingly, SelB contains an extended loop between β strands β25 and β26, which is considerably shorter in EF-Tu and EF-1A (Andersen *et al*, 2000; Vitagliano *et al*, 2001). This SelB region might be of functional importance for specific $tRNA^{Sec}$ recognition, because, based on the superposition with domain III in the

EF-Tu ternary complex (Nissen *et al*, 1995, 1999), it would interact with the uniquely long acceptor arm of $tRNA^{Sec}$.

SelB domain IV (residues 381–468) is implicated in either direct or adaptor-mediated recognition of the SECIS mRNA element. The overall topology of domain IV is a β barrel consisting of six β strands and a short α helix (α7) inserted between strands β29 and β30 (Figures 1A and 2). It is connected to domain III via a 20 Å long flexible linker. The linker consists of a short α helix (α6) and an antiparallel β sheet formed by the first and the last β strand (β28 and β33, respectively) of domain IV. A similarity search with the Cα chain of domain IV using the Dali server (www.ebi.ac.uk/dali/) revealed significant structural homologies with the N-terminal β barrel domain of F1-ATPase, EF-G domain II and, strikingly, domain IV of IF2 and eIF5B, although at the sequence level, the similarity to any of these domains is low.

Coupling of nucleotide exchange and tRNA binding in SelB

The comparison of the SelB:GDP and SelB:GppNHp structures revealed a shift of the Switch 2 region, which is part of domain I and is formed by residues 68–80, including helix α2 (Figures 2 and 3A). This conformational change was observed for one of the four molecules in the SelB:GppNHp crystal (molecule A) where the backbone electron density of this region is clearly visible. SelB domains II/III retain their 'GTP-like' arrangement relative to domain I upon nucleotide exchange, and the conformational change is restricted to the Switch 2 region. This is surprising because in EF-Tu, the shift of the Switch 2 region leads to a large movement of domains II/III as a rigid body relative to domain I (Berchtold *et al*, 1993; Kjeldgaard *et al*, 1993; Abel *et al*, 1996; Polekhina *et al*, 1996; Nissen *et al*, 1999), thereby increasing the affinity for the tRNA by four orders of magnitude (from 28 μM to 1 nM; Dell *et al*, 1990). This implicates that in SelB, the coupling of nucleotide exchange with Switch 2 and domain II/III movements is very different from EF-Tu.

In order to investigate how the tRNA binding and Switch 2 helix movement are coupled in SelB, we analysed the Switch 2 region of SelB:GDP in more detail. We found close contacts between the Switch 2 helix and loop β19–β20 of domain III in the SelB:GDP structure, which are absent in EF-Tu:GDP due to the large domain rearrangements upon nucleotide exchange and different in EF-Tu:GppNHp (Figure 3A; Abel *et al*, 1996; Polekhina *et al*, 1996; Nissen *et al*, 1999). These contacts are formed between residues Arg74/Ala75 from the Switch 2 helix and Met305/Ile307 from loop β19–β20 in domain III (Figures 2 and 3B). An additional contact is present between residues Arg74 and Arg262 (domain II), which together complex a sulphate anion. It is interesting that in the ternary EF-Tu complex, residues Lys90 and Arg300, corresponding to SelB Arg74 and Arg262, are directly involved in complexing the 5′ phosphate group of tRNA base G1, together with the neighbouring Asn91 (Ala75 in SelB; Nissen *et al*, 1999). In SelB:GDP, the set of interdomain contacts may prevent Arg74 and the neighbouring Ala75 from adopting a conformation that would allow efficient binding of the 5′ phosphate, thereby defining its 'OFF state' (Figure 3C). Upon GTP binding, Arg74/Ala75 should become released for contacting the tRNA 5′ phosphate, and this is exactly what is observed in the Switch 2 region of SelB:GppNHp (Figure 3A). The conformational change leads to a shift of the contact site between the domain III loop and the Switch 2 helix by one helix turn, now exposing Arg74 and Ala75 and defining the 'ON state' of SelB (Figure 3C). Altogether, this mechanism may explain how under physiological conditions SelB binds $Sec\text{-}tRNA^{Sec}$ only in its GTP state although there are no major conformational changes at the domain level between this and the GDP-bound states.

Conserved residues in the aminoacyl-binding pocket of SelB domain II are important for specific Sec recognition

The core of the aminoacyl-binding pocket from *M. maripaludis* SelB is formed by residues Asp191, His192 and Arg247, which are unique to SelB (Figures 2 and 4A). Asp191 and Arg247 are conserved among SelB molecules from all kingdoms, whereas His192 is present in archaeal and eukaryotic SelBs and is substituted by an Arg residue in most eubacterial SelBs (Figure 2). Residues His192 and Arg247 are especially intriguing because they introduce two positive charges into the aminoacyl-binding pocket and therefore might interact with the negatively charged selenol group (Figure 4A). In order to check for such an interaction, we superimposed SelB domain II with the corresponding domain from the EF-$Tu:GppNHp:tRNA^{Cys}$ complex (Nissen *et al*, 1999) and investigated the positioning of the sulphur atom from the cysteyl moiety, which would be similar to the selenol group in Sec (Figure 4B). Interestingly, residue Arg247 of SelB occupies the position of the corresponding Asn285 in EF-Tu, which is in direct contact with the 3′ cysteyl moiety in the ternary EF-Tu complex (Figure 4B). Therefore, Arg247 adds a positive charge at a critical position and is likely involved in compensating for the negative charge of the selenol group (Figure 4B). SelB residue His192 (Arg in most eubacterial SelBs) is localized similarly to the conserved Asp227 of EF-Tu, thereby replacing the negative charge in EF-Tu by a positive charge (Figure 4B). Based on these observations, we conclude that in SelB, either His192 or Arg247 would have the capacity to interact with the Se^- ion. However, it is also possible that

Figure 2 Secondary structure of SelB:GDP and structure-based alignment of selected SelB sequences from all kingdoms. Different SelB sequences from archaea, bacteria and eukaryotes were obtained from the NCBI protein sequence database (www.ncbi.nlm.nih.gov/Entrez/) and are depicted as follows: Mma, *M. maripaludis*; Mja, *M. jannaschii*; Mka, *Methanopyrus kandleri*; Cel, *Caenorhabditis elegans*; Dme, *Drosophila melanogaster*; Mmu, *Mus musculus*; Fru, *Fugu rubripes*; Eco, *E. coli* and Mth, *M. thermoacetica*. Domain borders are indicated in blue. Bacterial SelBs are truncated (depicted with (+)) after domain III due to the completely unrelated fold of domain IV. The alignment was performed using CLUSTAL X (Thompson *et al*, 1997) and edited manually with GeneDoc (www.psc.edu/biomed/genedoc). The colouring is according to the Gonnet PAM 250 series with 40% (yellow), 70% (orange) and 100% similarity (red). For comparison, the sequences of *Thermus aquaticus* EF-Tu (Taq), *Pyrococcus abyssi* IF2γ (Pab) and the core part of *Methanobacterium thermoautotrophicum* eIF5B domain IV are also aligned. The numbering of these sequences is according to the published structures. The zinc knuckle insertion in IF2γ domain I is depicted in green. Several important SelB residues are labelled according to their possible function: 5′ phosphate recognition (#), blocking of the 5′ recognition (x), aminoacyl binding (*) and tRNA backbone contacts (>). Mutations in residues affecting the interaction of murine SelB with SBP2 are depicted with (o). The Switch 1 and 2 regions are boxed in blue. The additional A′ helix and the thermophile loop (TL) in EF-Tu and the loop in eIF5B domain IV replaced by α7 in SelB are indicated in grey, between brackets.

both residues together are involved in complexing and stabilizing the reactive selenol group.

Another important amino-acid residue in SelB may be Phe51 (Tyr in some eubacterial SelBs). It is located in SelB domain I and protrudes into the aminoacyl-binding pocket of domain II, thereby causing a steric clash with the cysteyl moiety modelled into the binding pocket (Figure 4C). As a consequence, this residue would have to move out of the pocket when Sec binds. The inherent flexibility of Phe51 suggests that this hydrophobic residue could serve as a lid

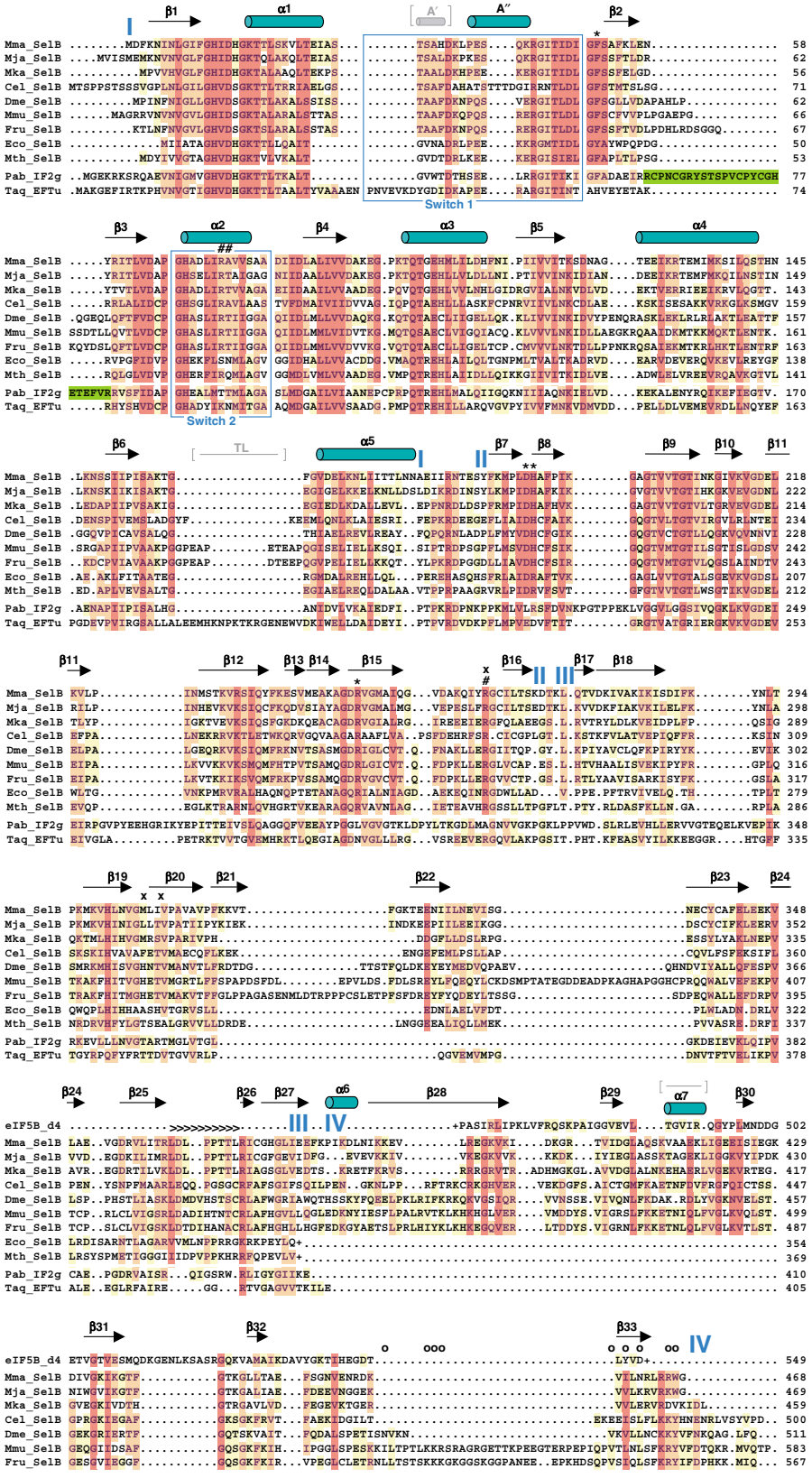

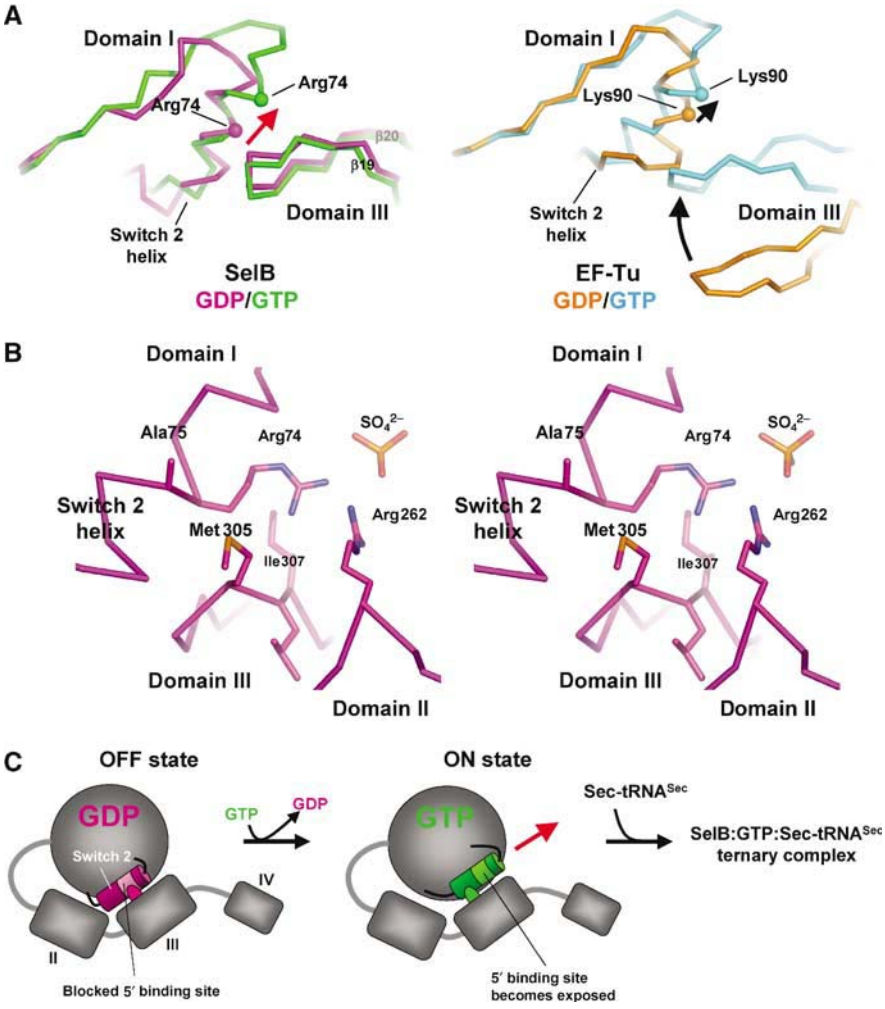

Figure 3 Conformational changes in the Switch 2 region of SelB domain I induced by GppNHp binding lead to the exposure of residues proposed to be involved in clamping the 5′ phosphate of the tRNA. (**A**) Comparison of the GDP and GTP conformations of SelB (molecule A, left) and EF-Tu (right). In SelB, nucleotide exchange leads to a conformational change restricted to the Switch 2 helix. Domains II, III and IV retain their relative positions, whereas the contact between domain III and Switch 2 is shifted by one helix turn (red arrow). EF-Tu, in contrast, undergoes large conformational changes that include, in addition to Switch 2, the movement of domain III towards the Switch 2 helix (black arrows). (**B**) Stereo view of the Switch 2 helix in contact with domains II and III from SelB:GDP (molecule C). Switch 2 residues Arg74 and Ala75 that may be involved in clamping the tRNA 5′ phosphate are blocked by several contacts with residues from domains II and III. (**C**) Model of the coupling between nucleotide and tRNA binding in SelB. In spite of adopting an overall 'GTP-like' conformation, SelB:GDP binds tRNA with lower affinity because the 5′ phosphate binding site is blocked by domain III (left). Upon GTP binding, the movement of the Switch 2 helix by one helix turn leads to the exposure of the tRNA-binding site and the formation of a ternary complex.

to protect the highly reactive Sec from oxidation. This is different from EF-Tu:GppNHp, where the corresponding His67 residue (Figure 4C) does not change location upon tRNA binding (Berchtold *et al*, 1993; Kjeldgaard *et al*, 1993; Nissen *et al*, 1999).

In order to analyse the importance of Phe51, His192 and Arg247, we introduced point mutations at the corresponding positions in *E. coli* SelB. Asp191 was also tested due to its strict conservation among all SelBs. The amino acids in *E. coli* SelB were mutated to the corresponding EF-Tu residues (Tyr42→His42, Asp180→Glu180, Arg181→Asp181 and Arg236→Asn236) in order to not only abolish the binding of Sec-tRNA^{Sec}, but also to promote the binding of Ser-tRNA^{Sec}, which is rejected by wild-type SelB. Ser-tRNA^{Sec} recognition was tested by transferring SelB alleles carrying single mutations or combinations of these into *E. coli* strain AF90422/pWT, which is unable both to synthesize SelB and to convert Ser-tRNA^{Sec} into Sec-tRNA^{Sec} due to deletion of the *selAB* operon (Materials and methods, Supplementary data and Table II). Similarly, recognition of Sec-tRNA^{Sec} was analysed in strain PT91300/pWT, which possesses a functional *selA* gene product but lacks the *selB* gene. As a screening system, readthrough of an in-frame UGA codon that interrupts the reading frame of a *lacZ* reporter gene and that is followed by the SECIS sequence of the *E. coli* formate dehydrogenase H (*fdhF*) gene was assayed (Figure 4D). The β-galactosidase activities measured for the respective transformants are listed in Table II.

Surprisingly, only a single variant containing the three mutations Tyr42→His42/Asp180→Glu180/Arg236→Asn236 slightly increased Ser-tRNA^{Sec} readthrough activity. All the other mutants were less active than wild-type SelB.

The majority of the variants were fully functional in the presence of Sec-tRNA^{Sec} or exhibited even slightly higher

activity. Single replacements of Arg181→Asp181 or Arg236→Asn236 (corresponding to His192 and Arg247 in our SelB structure) did not affect SelB activity significantly. Strikingly, all variants in which both amino acids were exchanged had lost their functionality. In addition, the readthrough activity was greatly reduced in the case of the Asp180→Glu180/Arg181→Asp181 double mutation. To check whether the loss of function might be caused by instability of SelB, the transformants were tested with anti-SelB antibodies (Figure 4D). All 15 transformants, however, had comparable SelB levels. Therefore, it appears that the presence of at least one positive charge in the aminoacyl-binding pocket of SelB is required for function with Sec-tRNA^{Sec}. Removal of both positive charges, however, does not confer the capacity to accept Ser-tRNA^{Sec} as a ligand. Taken together, all these observations confirm the importance of Phe51, Asp191, His192 and Arg247 for specific binding of Sec-tRNA^{Sec}.

Recognition of the tRNA backbone

SelB domain III contains an extended loop (Leu361-Asp-Leu-Pro-Pro-Thr-Thr-Leu368, located between β25 and β26) that is strictly conserved among archaea and may be present also in eukaryotes and eubacteria, although in eubacteria, a precise alignment of this region is difficult to perform due to low sequence similarity (Figures 2 and 5A). Interestingly, the corresponding loop is considerably shorter in all EF-1A and EF-Tu structures available so far. In the ternary EF-Tu complex, it forms an important, nonspecific backbone contact with the tRNA (Figures 2 and 5A; Nissen *et al*, 1999). Superimposing SelB domain III onto EF-Tu in complex with Cys-tRNA^{Cys} allowed us to investigate possible interactions with the tRNA backbone (Figure 5A). Based on this superposition, the SelB extension is able to contact a large tRNA area, including residues C51, G52, G53, C62, G63, G64 and A65, which form base pairs 8–12 of the tRNA^{Cys} acceptor arm (Figure 5A). Therefore, SelB would be able to contact the elbow region of canonical tRNAs. Assuming that the acceptor arm of tRNA^{Sec} forms a prolonged regular helix, the corresponding bases in the secondary structure diagram of

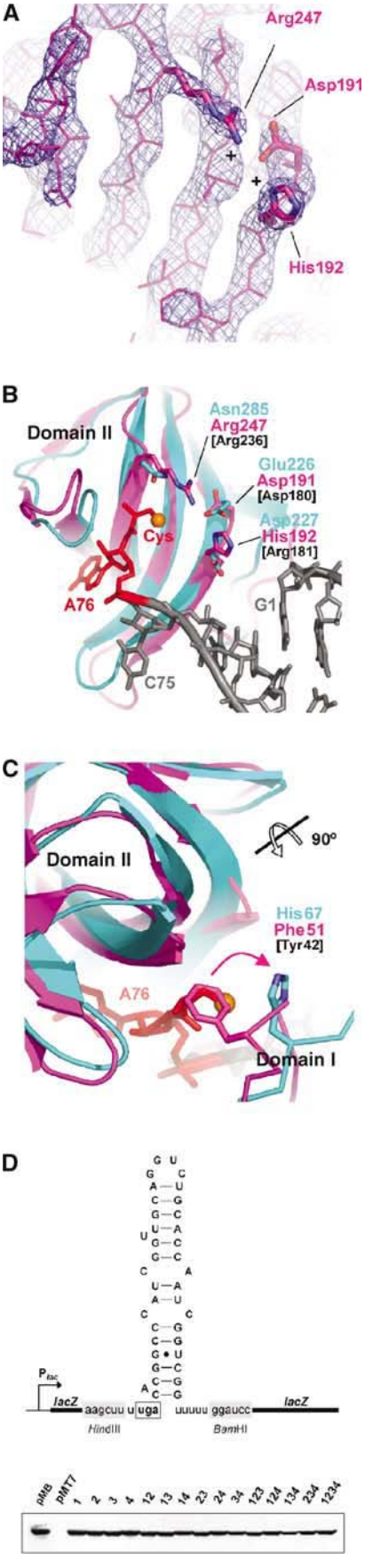

Figure 4 Aminoacyl-binding pocket of SelB and superposition with the corresponding EF-Tu:GppNHp:Cys-tRNA^{Cys} region. *M. maripaludis* SelB is coloured in magenta, EF-Tu in cyan, the tRNA in grey and its terminal 3′Cys-A76 in red. Amino acids of *E. coli* SelB that in the mutational analysis were replaced by the corresponding EF-Tu residues are labelled in black. (**A**) $2F_o-F_c$ electron density map of the aminoacyl-binding pocket from SelB molecule C, contoured at 2.5 σ. Two positively charged residues (Arg247 and His192) may compensate for the negatively charged selenium. (**B, C**) Superposition of SelB and EF-Tu demonstrating the differences between key residues involved in aminoacyl binding. As a reference, the sulphur atom of the cysteyl moiety is displayed as an orange sphere. In SelB, Phe51 from domain I protrudes into the aminoacyl-binding pocket, thereby occupying the position of the modelled cysteyl side chain. (**D**) Mutational analysis of the aminoacyl-binding pocket from *E. coli* SelB. A scheme of the *lacZ* reporter gene carried by plasmid pWT is shown in the upper panel. The sequence of the UGA-SECIS cassette inserted into the 5′ portion of *lacZ* is depicted as mRNA sequence in its predicted secondary structure. The fusion gene is transcribed from the *lac* promoter (P_{lac}). In the lower panel, an immunoblot analysis of cells expressing SelB variants with exchanges in the aminoacyl-binding pocket is shown as a control. Aliquots of cells used to determine the β-galactosidase activities listed in Table II were lysed and probed with anti-SelB antiserum. The numbering of the lanes relates to the numbering of the respective plasmids as given in Table II.

Table II UGA readthrough activity of *E. coli* SelB variants containing amino-acid exchanges in the aminoacyl-tRNA-binding pocket[a]

Plasmid	Mutations	Readthrough activity (Miller units) with	
		Ser-tRNA^{Sec}	Sec-tRNA^{Sec}
pMB	Wild type	8.9	273.4
pMT7	Empty vector	1.5	0.6
pMBD-1	Y42H	7.9	397.7
pMBD-2	D180E	4.4	375.7
pMBD-3	R181D	0.8	232.0
pMBD-4	R236N	6.2	334.0
pMBD-12	Y42H, D180E	3.1	469.4
pMBD-13	Y42H, R181D	1.0	336.4
pMBD-14	Y42H, R236N	4.2	163.8
pMBD-23	D180E, R181D	0.5	15.2
pMBD-24	D180E, R236N	6.0	495.1
pMBD-34	R181D, R236N	0.5	0.7
pMBD-123	Y42H, D180E, R181D	0.9	214.9
pMBD-124	Y42H, D180E, R236N	21.8	544.2
pMBD-134	Y42H, R181D, R236N	0.4	0.0
pMBD-234	D180E, R181D, R236N	0.7	0.2
pMBD-1234	Y42H, D180E, R181D, R236N	0.9	1.4

[a]Control plasmids or plasmids bearing mutated *selB* alleles were transferred into AF90422/pWT and PT91300/pWT to measure UGA readthrough with Ser-tRNA^{Sec} and Sec-tRNA^{Sec}, respectively, and β-galactosidase activities were determined. The results of at least three independent experiments, each of which was performed in triplicate, were averaged.

M. maripaludis tRNA^{Sec} would form the last two base pairs of the acceptor stem and the first three base pairs of the T stem (G6–C67/G7–C66/G50–C64/G51–C63 and G52–C62, respectively; Figure 5B). In principle, the loop in SelB domain III would even be long enough to contact the last base pair of the extra long tRNA^{Sec} acceptor arm (G53–C61) if it adopts an extended conformation upon tRNA binding. In this case, SelB would essentially measure the length of the acceptor arm and select against the shorter canonical tRNAs.

Discussion

Interaction of SelB with Sec-tRNA^{Sec}

Both SelB and IF2γ specifically recognize unique tRNAs, a situation that differs from the general tRNA recognition by EF-Tu. This additional layer of specificity can be achieved via recognition of the aminoacyl moiety and/or unique features of the tRNA (Commans and Böck, 1999; Kapp and Lorsch, 2004).

As a consequence, residues forming the aminoacyl-binding pockets of SelBs and IF2γs are significantly different from those encountered in EF-Tu (Schmitt *et al*, 2002; Roll-Mecak *et al*, 2004). In SelB, the pocket contains two positively charged residues, which likely compensate for the negative charge of the selenol group (Figure 4A). Furthermore, the reactive selenium may be shielded from the environment by Phe51, which might close the pocket after Sec-tRNA^{Sec} has bound to SelB (Figure 4C). The importance of several residues for Sec binding was further corroborated by our mutational analysis (Table II). In fact, only a combination of point mutations leads to a loss of function, and the specificity of SelB for Sec-tRNA^{Sec} cannot be easily changed towards Ser-tRNA^{Sec}. This is an indication of a complex recognition mechanism, which may also include subtle structural changes transmitted to the acceptor arm of the tRNA and/or to other regions of SelB upon binding of the selenol group.

In domain III of our SelB structure (Figure 5A), we found a loop considerably extended in comparison to EF-Tu, where it mediates an important unspecific contact with the backbone of the tRNA acceptor arm (Nissen *et al*, 1995, 1999). According to our model, this loop may contact the elbow region in the acceptor arm of tRNA^{Sec}. So far, this SelB region has escaped detection by alignment, probably due to low sequence homology with EF-Tu, and has not been investigated yet. The strict conservation of the loop in archaea and its presence in other species may be an indication of its importance. Furthermore, several types of amino acids found in this loop are known to be involved in RNA binding in general (Klein *et al*, 2004). For specific tRNA^{Sec} recognition, the detection of the extra base pair present in tRNA^{Sec} would be the simplest way. This would also explain why eukaryotic tRNA^{Sec} substitutes for the bacterial counterpart in *E. coli*, in spite of considerable sequence differences (Baron *et al*, 1994). It is also possible that the corresponding domain III loop in archaeal IF2γ (Schmitt *et al*, 2002; Roll-Mecak *et al*, 2004), which is shorter than in SelB but longer than in EF-Tu, may be involved in specific binding of IF2γ to its cognate tRNA$_i^{Met}$.

The amino-acid residues involved in clamping the 5′ phosphate of the canonical tRNAs in EF-Tu are partially conserved in SelB. Furthermore, the first base pair of tRNA^{Sec} is G1–C72, which is common for many elongator tRNAs. This suggests that SelB binds the tRNA^{Sec} 5′ phosphate in a manner similar to EF-Tu. The residues in the Switch 2 helix that may be critical for the interaction with the 5′ phosphate are blocked in the SelB:GDP structure by tight contacts with domains II and III. Consequently, in order to bind tRNA^{Sec}, these residues have to be released. We observed a GppNHp-induced movement of the Switch 2 helix in one of the SelB:GppNHp molecules in the crystal, leading to the exposure of these residues (Figure 3A). However, two other noncrystallographically related molecules were found to be in the SelB-apo form, whereas a fourth, although GppNHp-bound, retained the GDP conformation of Switch 2. This may be an indication that the Switch 2 GDP and GTP conformations are energetically very close.

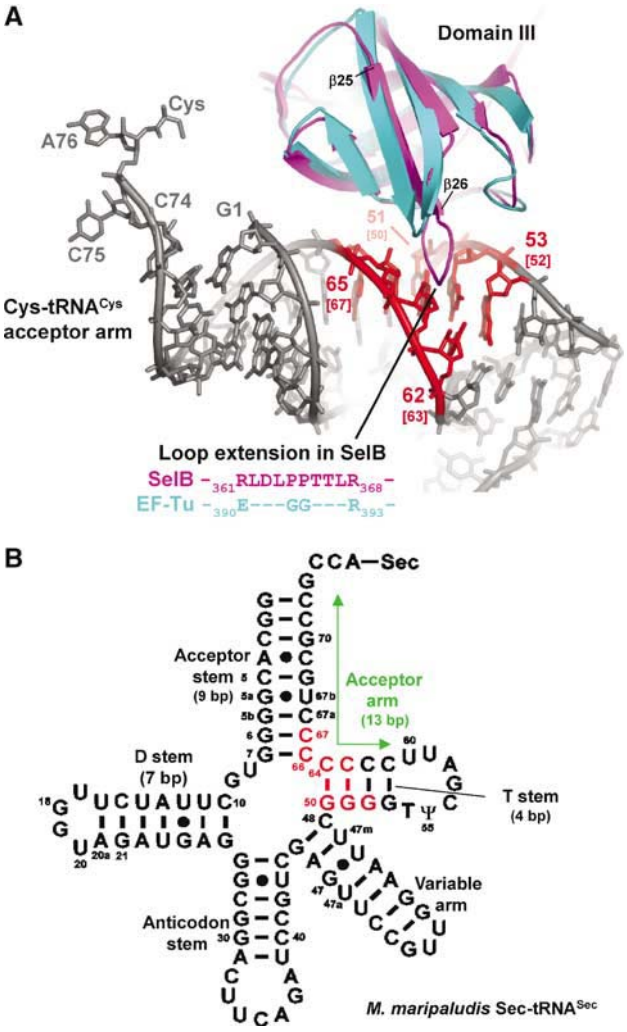

Figure 5 Superposition of SelB domain III with the corresponding EF-Tu domain, which is involved in a tRNA backbone contact. (**A**) SelB (magenta) contains a loop that is considerably extended in comparison with EF-Tu (cyan), where this region is involved in tRNA (grey) binding. Contacts between SelB and the modelled $tRNA^{Cys}$ are coloured in red. The base-pair numbering is according to $tRNA^{Cys}$. In addition, the corresponding bases from *M. maripaludis* $tRNA^{Sec}$ are shown in brackets. (**B**) Possible contact sites of SelB with $tRNA^{Sec}$ are shown in the secondary structure diagram of *M. maripaludis* Sec-$tRNA^{Sec}$ and are coloured in red. The contact area is derived from the $tRNA^{Cys}$:SelB model. Note the prolonged 13 bp acceptor arm (labelled with a green arrow) that is formed by stacking of the 9 bp acceptor stem and the 4 bp T stem and is an important difference when compared to canonical elongator tRNAs.

Considering that archeal SelB has low affinities for both nucleotides (K_d of 0.4 μM for GDP and 0.1 μM for GTP; Rother *et al*, 2000), it is reasonable to assume that GTP binding unlocks the Switch 2 helix for clamping the 5′ phosphate of the tRNA. However, for a stable Switch 2 GTP conformation, a concerted binding of the tRNA 5′ phosphate may be necessary.

The other part of SelB domain I that may adopt alternative conformations after nucleotide exchange is the Switch 1 region. In one of the SelB molecules, this region is visible but it is placed away from domain I and stabilized by interactions with a neighbouring molecule in the crystal lattice. Probably, the Switch 1 region is flexible and adopts a discrete conformation only upon $tRNA^{Sec}$ or ribosome binding.

Function of SelB domain IV

In bacterial SelB, domain IV is responsible for the direct interaction with the SECIS element (Kromayer *et al*, 1996; Fourmy *et al*, 2002). In contrast, eukaryotic SelB domain IV interacts with SBP2, which serves as an adaptor protein and binds both the SECIS element and domain IV (Allmang *et al*, 2002; Zavacki *et al*, 2003). The structural homology between domains IV of *M. maripaludis* SelB and *M. thermoautotrophicum* IF2/eIF5B (Figure 6B; Roll-Mecak *et al*, 2000) or *B. stearothermophilus* IF2 (Meunier *et al*, 2000) and the observation that domain IV of bacterial IF2 binds RNA (Guenneugues *et al*, 2000) suggest that domain IV in archeal SelB is involved in RNA binding, although this has not been demonstrated yet (Rother *et al*, 2000). It could directly recognize the SECIS element as observed in bacteria, and not via an adapter protein, as it is the case in eukaryotes. This would also be consistent with the observation that the C-terminal region of domain IV, which is responsible for the interaction with SBP2 in eukaryotes (Zavacki *et al*, 2003), is considerably shorter in archaeal SelB sequences (Figure 2). Furthermore, our attempts to find an archeal functional or sequence homologue of SBP2 have not been successful so far.

The observation that the C-terminal domain from *M. maripaludis* is structurally completely unrelated to the one from *Moorella thermoacetica* (Selmer and Su, 2002) suggests that bacterial and archeal SelB domains IV have evolved convergently. Although the structure of bacterial domain IV has been solved in isolation, it is not clear whether the positioning of this domain relative to the rest of the factor will resemble the one observed in archaeal SelB presented here. Domains IV in bacteria and archaea could have been acquired independently and may have adapted in parallel for the recoding of the composite Sec codon during evolution. In the eukaryotic translation machinery, SelB may have lost its original capacity for direct SECIS binding as it acquired an adapter protein. Such an adaptation is probably necessary due to the large distances between the internal stop codons and eukaryotic SECIS elements.

Structural similarity with eIF5B

Analysing the results from the Dali structural similarity search, we were surprised to find that not only domain IV of initiation factor IF2/eIF5B showed structural homology with the corresponding domain of the SelB molecule, but that additionally both molecules adopt a similar overall domain arrangement referred to as a 'molecular chalice' (Figure 6A; Roll-Mecak *et al*, 2000). Furthermore, domains I and II of the two factors are homologous as it is the case for many G proteins involved in translation. This structural similarity at the level of overall shape raises the question of parallels between initiation and elongation via 'antitermination', which are not immediately obvious.

During eukaryotic translation initiation, eIF5B:GTP promotes the joining of the large ribosomal subunit by binding to the small subunit, which carries the eIF2αβγ:GTP:$tRNA_i^{Met}$ complex in the P site and eIF1A in the A site (Pestova *et al*, 2000; Shin *et al*, 2002). Upon assembly of the 80S ribosome, the release of eIF5B:GDP from the ribosome is thought to be

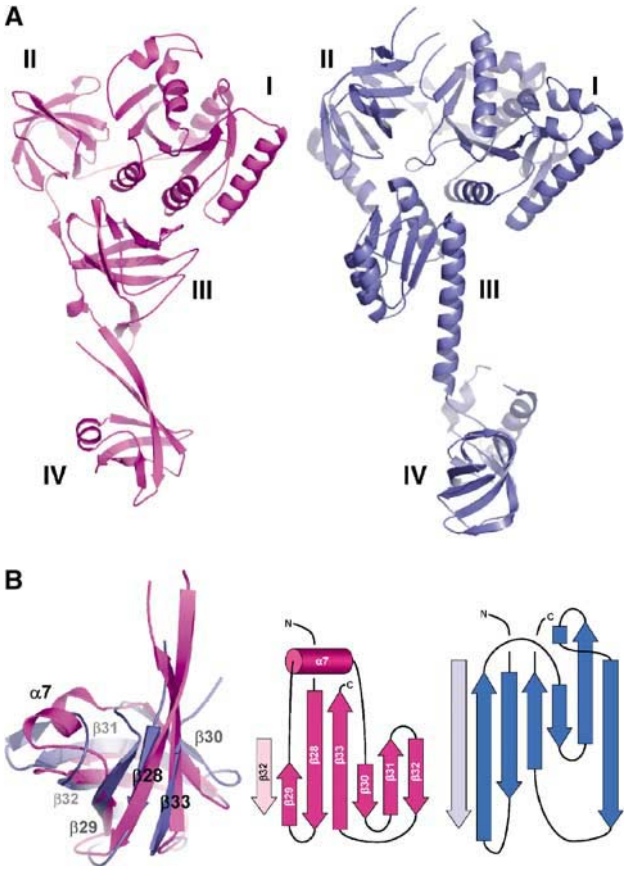

Figure 6 'Molecular chalice' shape of both SelB from *M. maripaludis* (magenta) and eIF5B from *M. thermoautotrophicum* (blue). (**A**) SelB:GDP and eIF5B:GDP are similar in size and show a comparable overall domain arrangement. This structural homology may indicate a related mode of interaction with the ribosome. (**B**) Superposition of SelB domain IV with the β barrel core from eIF5B domain IV. The topologies of both domains are closely related despite their low sequence homology. However, the SelB α7 helix substitutes for a loop observed in eIF5B (middle and right).

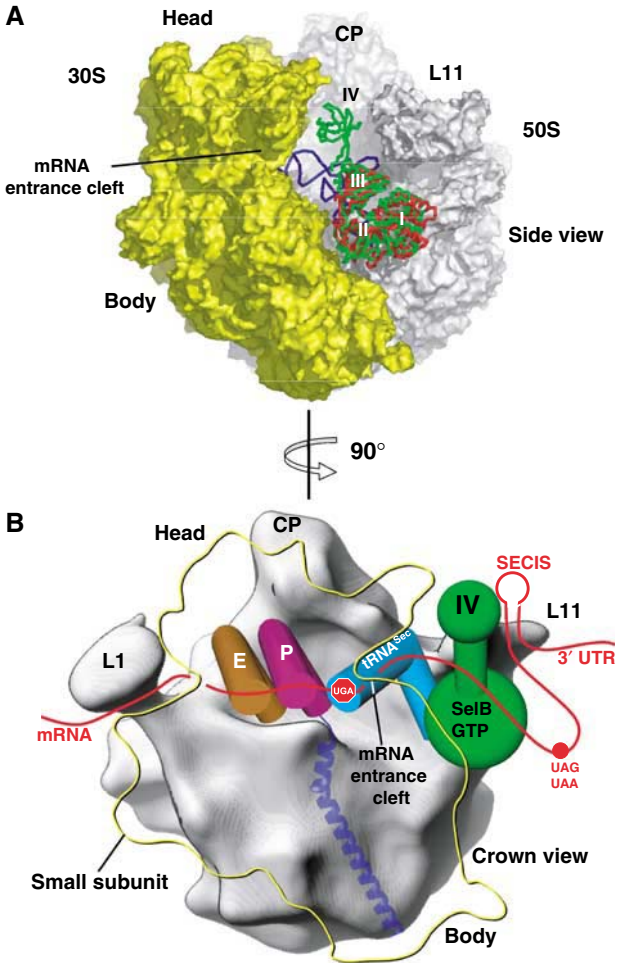

Figure 7 Model of SelB bound to the GTPase activating centre of the 70S ribosome prior to the release of the tRNA. (**A**) Superposition of SelB domains I–III with the corresponding domains from the EF-Tu:GDP:Phe-tRNA^{Phe}:kirromycin complex bound to the 70S ribosome. After superposition of SelB (green) with EF-Tu (red), SelB domain IV points towards the mRNA entrance cleft of the small ribosomal subunit. The A/T state Phe-tRNA^{Phe} from the EF-Tu complex is depicted in blue. CP: central protuberance; L11: L11 region of the large subunit. (**B**) In the schematic representation, the crown view of the 50S subunit is shown (grey). Domain IV of SelB (green), which points towards the mRNA entrance cleft formed by the 30S subunit (yellow outline), would allow SelB to bind the SECIS element located in the 3′ UTR of the mRNA (red) either directly or via an adapter protein. Sec-tRNA^{Sec} (blue) bound to SelB:GTP would recognize the internal UGA stop codon located in the A site of the small ribosomal subunit (shown as 'stop signal'). The usual UAA or UAG stop codon of the gene is indicated with a red dot, and the tRNAs located in the P and E sites are depicted in magenta and brown, respectively. L1: large ribosomal protein L1; CP: central protuberance; L11: L11 region of the large subunit.

triggered by GTP hydrolysis, thereby leaving a ribosome competent for elongation. During this process, domain IV of eIF5B binds to IF1A with a C-terminal domain IV extension that is not present in SelB (Marintchev *et al*, 2003; Olsen *et al*, 2003).

The remarkable similarity of domains IV and of the overall molecular shape between SelB and eIF5B raises questions of whether the two factors interact with a common set of spatially separated binding sites on the translating ribosome and whether their domains IV have a related function. Like SelB, domain IV of eIF5B may be contacting directly or indirectly the mRNA, thereby preventing linear diffusion of the initiation complex away from the start codon following the release of eIF2αβγ. Interestingly, Kozak (1990) observed that downstream secondary hairpin structures in the mRNA facilitate the recognition of start codons in a suboptimal context. Such an interaction would only be possible if domain IV is projected towards the mRNA entrance site on the 30S subunit, which would not exclude the observed interactions with eIF1A mediated via the unstructured C-terminal tail of eIF1A that could extend more than 70 Å in length (Marintchev *et al*, 2003). Under the reasonable assumption that initiation factor eIF5B and elongation factors EF-Tu and SelB bind to the GTPase centre of the 70S ribosome in a similar manner, domains IV of eIF5B and SelB are optimally positioned for the interaction with mRNA, as discussed in the next section.

Model of SelB bound to the ribosome

Valle *et al* (2003) investigated the structure of EF-Tu in complex with GppNHp, Phe-tRNA^{Phe} and kirromycin on the 70S ribosome by cryo-electron microscopy and interpreted

the 3D reconstructions using the high-resolution structures. This conformational state of the ribosome corresponds to the situation when SelB:GTP:Sec-tRNA^{Sec} ternary complex is bound to the GTPase activating centre of the large subunit and interacts with the UGA Sec codon in the decoding centre of the small subunit via the Sec-tRNA^{Sec} UCA anticodon. Furthermore, at the pretranslocation state of the elongation cycle, SelB should be in contact with the SECIS element, thereby receiving the recoding signal. In order to visualize the approximate positioning of SelB domain IV with respect to the ribosome at this state of the elongation cycle, we superimposed domains I–III with the corresponding ribosome-bound EF-Tu domains (Figure 7A). According to this modelling, domain IV of SelB points towards the mRNA entrance cleft, formed by the small ribosomal subunit, and is optimally positioned to recognize the SECIS element (Figure 7B).

Conclusions and outlook

The SelB structure from *M. maripaludis* revealed a translation elongation factor that is an EF-Tu/eIF2γ/IF2/eIF5B hybrid molecule. This raises interesting questions: What are the similarities between Sec incorporation and initiation? How did these two processes evolve and how are they related to the EF-Tu/EF-G-mediated elongation? Additionally, the Sec incorporation could be mechanistically analogous to the recently discovered process of cotranslational incorporation of the 22nd amino acid pyrrolysine into proteins through recoding of the UAG (amber) stop codon (Ibba and Söll, 2002). The structure of SelB described here offers a good starting point for future investigation of Sec incorporation and the other related translational processes by a combination of genetic, biochemical and structural approaches in all three descents.

Materials and methods

Protein purification, crystallization and structure determination

An N-terminally His-tagged version of SelB was purified using standard procedures. The protein was crystallized by the vapour diffusion method from ammonium sulphate either in the presence of GDP, GppHNp or without nucleotide, yielding isomorphous crystals for all three forms. Alternatively, crystals of SelB-apo and SelB:GppHNp with better diffraction properties were obtained from SelB:GDP-grown crystals by either omitting GDP from or adding GppNHp to the stabilization solution. This procedure was validated by inspection of F_o–F_o difference Fourier maps between the data sets. All crystals were derivatized with methyl mercury during stabilization and flash-frozen.

Hg SAD data were collected remote of the Hg L-III absorption edge. The data were processed with HKL (Otwinowski and Minor, 1997). Experimental Hg SAD phases were obtained using CNS for phasing and solvent flipping (Brünger *et al*, 1998). The SelB:GDP model was built manually into the electron density map using O (Jones *et al*, 1991) and was refined and completed by rebuilding into difference Fourier maps. The structures of SelB:GppNHp and SelB-apo were solved using the atomic coordinates of SelB:GDP as a starting model.

Mutational analysis of E. coli SelB

Point mutations were introduced into a His-tagged *E. coli selB* allele carried on a plasmid by inverse PCR. After transferring the mutated alleles into Δ*selAB* or Δ*selB* strains bearing the *lacZ* reporter gene, the cells were grown to an OD_{600} of ~1.5 and the β-galactosidase activities were measured. For the SelB expression tests, proteins from the different cultures were separated by SDS–PAGE. SelB was detected by Western blot using affinity-purified anti-SelB antibodies and chemiluminescence detection.

Detailed descriptions of Materials and methods are available online as Supplementary data.

Coordinates

The coordinates are deposited in the PDB under accession numbers 1wb1 (SelB:GDP), 1wb2 (SelB-apo) and 1wb3 (Selb:GppNHp).

Supplementary data

Supplementary data are available at *The EMBO Journal* Online.

Acknowledgements

Data collection was performed at the Swiss Light Source (SLS) of the Paul Scherrer Institut (PSI) in Villigen. We are grateful to C Schulze-Briese, T Tomizaki and A Wagner at the SLS whose outstanding efforts have made these experiments possible. This work was supported by the Swiss National Science Foundation (SNSF), the NCCR Structural Biology program of the SNSF, the ETH internal research grant TH-1/01-2, and a Young Investigator grant from the Human Frontier Science Program to NB.

References

Abel K, Yoder MD, Hilgenfeld R, Jurnak F (1996) An α to β conformational switch in EF-Tu. *Structure* **4:** 1153–1159

Ævarsson A, Brazhnikov E, Garber M, Zheltonosova J, Chirgadze Y, al-Karadaghi S, Svensson LA, Liljas A (1994) Three-dimensional structure of the ribosomal translocase: elongation factor G from *Thermus thermophilus*. *EMBO J* **13:** 3669–3677

Allmang C, Carbon P, Krol A (2002) The SBP2 and 15.5 kD/Snu13p proteins share the same RNA binding domain: identification of SBP2 amino acids important to SECIS RNA binding. *RNA* **8:** 1308–1318

Andersen GR, Pedersen L, Valente L, Chatterjee I, Kinzy TG, Kjeldgaard M, Nyborg J (2000) Structural basis for nucleotide exchange and competition with tRNA in the yeast elongation factor complex eEF1A:eEF1Bα. *Mol Cell* **6:** 1261–1266

Atkins JF, Gesteland RF (2000) The twenty-first amino acid. *Nature* **407**, 463, 465

Baron C, Böck A (1991) The length of the aminoacyl-acceptor stem of the selenocysteine-specific tRNA^{Sec} of *Escherichia coli* is the determinant for binding to elongation factors SELB or Tu. *J Biol Chem* **266:** 20375–20379

Baron C, Böck A (1995) The selenocysteine-inserting tRNA species: structure and function. In *tRNA: Structure, Biosynthesis, and Function*, Söll D, RajBhandary UL (eds) pp 529–544. Washington, DC: ASM Press

Baron C, Sturchler C, Wu XQ, Gross HJ, Krol A, Böck A (1994) Eukaryotic selenocysteine inserting tRNA species support selenoprotein synthesis in *Escherichia coli*. *Nucleic Acids Res* **22:** 2228–2233

Baron C, Westhof E, Böck A, Giege R (1993) Solution structure of selenocysteine-inserting tRNA^{Sec} from *Escherichia coli*. Comparison with canonical tRNA^{Ser}. *J Mol Biol* **231:** 274–292

Berchtold H, Reshetnikova L, Reiser CO, Schirmer NK, Sprinzl M, Hilgenfeld R (1993) Crystal structure of active elongation factor Tu reveals major domain rearrangements. *Nature* **365:** 126–132

Berry MJ, Banu L, Chen YY, Mandel SJ, Kieffer JD, Harney JW, Larsen PR (1991) Recognition of UGA as a selenocysteine codon in type I deiodinase requires sequences in the 3′ untranslated region. *Nature* **353:** 273–276

Brünger AT, Adams PD, Clore GM, DeLano WL, Gros P, Grosse-Kunstleve RW, Jiang JS, Kuszewski J, Nilges M, Pannu NS, Read RJ, Rice LM, Simonson T, Warren GL (1998) Crystallography & NMR system: a new software suite for macromolecular structure determination. *Acta Crystallogr D* **54:** 905–921

Commans S, Böck A (1999) Selenocysteine inserting tRNAs: an overview. *FEMS Microbiol Rev* **23:** 335–351

Copeland PR, Fletcher JE, Carlson BA, Hatfield DL, Driscoll DM (2000) A novel RNA binding protein, SBP2, is required for the translation of mammalian selenoprotein mRNAs. *EMBO J* **19:** 306–314

Czworkowski J, Wang J, Steitz TA, Moore PB (1994) The crystal structure of elongation factor G complexed with GDP, at 2.7 Å resolution. *EMBO J* **13:** 3661–3668

Dell VA, Miller DL, Johnson AE (1990) Effects of nucleotide- and aurodox-induced changes in elongation factor Tu conformation upon its interactions with aminoacyl transfer RNA. A fluorescence study. *Biochemistry* **29:** 1757–1763

Fagegaltier D, Hubert N, Yamada K, Mizutani T, Carbon P, Krol A (2000) Characterization of mSelB, a novel mammalian elongation factor for selenoprotein translation. *EMBO J* **19:** 4796–4805

Forchhammer K, Leinfelder W, Böck A (1989) Identification of a novel translation factor necessary for the incorporation of selenocysteine into protein. *Nature* **342:** 453–456

Förster C, Ott G, Forchhammer K, Sprinzl M (1990) Interaction of a selenocysteine-incorporating tRNA with elongation factor Tu from *E. coli*. *Nucleic Acids Res* **18:** 487–491

Fourmy D, Guittet E, Yoshizawa S (2002) Structure of prokaryotic SECIS mRNA hairpin and its interaction with elongation factor SelB. *J Mol Biol* **324:** 137–150

Guenneugues M, Caserta E, Brandi L, Spurio R, Meunier S, Pon CL, Boelens R, Gualerzi CO (2000) Mapping the fMet-tRNA^{fMet} binding site of initiation factor IF2. *EMBO J* **19:** 5233–5240

Hatfield DL (2001) *Selenium: Its Molecular Biology and Role in Human Health*. Boston/Dordrecht/London: Kluwer Academic Publishers

Hilgenfeld R, Böck A, Wilting R (1996) Structural model for the selenocysteine-specific elongation factor SelB. *Biochimie* **78:** 971–978

Hill KE, Lloyd RS, Burk RF (1993) Conserved nucleotide sequences in the open reading frame and 3′ untranslated region of selenoprotein P mRNA. *Proc Natl Acad Sci USA* **90:** 537–541

Hubert N, Sturchler C, Westhof E, Carbon P, Krol A (1998) The 9/4 secondary structure of eukaryotic selenocysteine tRNA: more pieces of evidence. *RNA* **4:** 1029–1033

Ibba M, Söll D (2002) Genetic code: introducing pyrrolysine. *Curr Biol* **12:** R464–R466

Jones TA, Zou JY, Cowan SW, Kjeldgaard M (1991) Improved methods for building protein models in electron density maps and the location of errors in these models. *Acta Crystallogr A* **47:** 110–119

Kapp LD, Lorsch JR (2004) GTP-dependent recognition of the methionine moiety on initiator tRNA by translation factor eIF2. *J Mol Biol* **335:** 923–936

Keeling PJ, Fast NM, McFadden GI (1998) Evolutionary relationship between translation initiation factor eIF-2γ and selenocysteine-specific elongation factor SELB: change of function in translation factors. *J Mol Evol* **47:** 649–655

Kjeldgaard M, Nissen P, Thirup S, Nyborg J (1993) The crystal structure of elongation factor EF-Tu from *Thermus aquaticus* in the GTP conformation. *Structure* **1:** 35–50

Klein DJ, Moore PB, Steitz TA (2004) The roles of ribosomal proteins in the structure assembly, and evolution of the large ribosomal subunit. *J Mol Biol* **340:** 141–177

Kozak M (1990) Downstream secondary structure facilitates recognition of initiator codons by eukaryotic ribosomes. *Proc Natl Acad Sci USA* **87:** 8301–8305

Kromayer M, Wilting R, Tormay P, Böck A (1996) Domain structure of the prokaryotic selenocysteine-specific elongation factor SelB. *J Mol Biol* **262:** 413–420

Kyriakopoulos A, Behne D (2002) Selenium-containing proteins in mammals and other forms of life. *Rev Physiol Biochem Pharmacol* **145:** 1–46

Marintchev A, Kolupaeva VG, Pestova TV, Wagner G (2003) Mapping the binding interface between human eukaryotic initiation factors 1A and 5B: a new interaction between old partners. *Proc Natl Acad Sci USA* **100:** 1535–1540

Meunier S, Spurio R, Czisch M, Wechselberger R, Guenneugues M, Gualerzi CO, Boelens R (2000) Structure of the fMet-tRNA^{fMet}-binding domain of *B. stearothermophilus* initiation factor IF2. *EMBO J* **19:** 1918–1926

Nissen P, Kjeldgaard M, Thirup S, Polekhina G, Reshetnikova L, Clark BF, Nyborg J (1995) Crystal structure of the ternary complex of Phe-tRNA^{Phe}, EF-Tu, and a GTP analog. *Science* **270:** 1464–1472

Nissen P, Thirup S, Kjeldgaard M, Nyborg J (1999) The crystal structure of Cys-tRNA^{Cys}-EF-Tu-GDPNP reveals general and specific features in the ternary complex and in tRNA. *Struct Fold Des* **7:** 143–156

Olsen DS, Savner EM, Mathew A, Zhang F, Krishnamoorthy T, Phan L, Hinnebusch AG (2003) Domains of eIF1A that mediate binding to eIF2, eIF3 and eIF5B and promote ternary complex recruitment *in vivo*. *EMBO J* **22:** 193–204

Otwinowski Z, Minor W (1997) Processing X-ray diffraction data collected in oscillation mode. *Methods Enzymol* **276:** 307–326

Pestova TV, Lomakin IB, Lee JH, Choi SK, Dever TE, Hellen CU (2000) The joining of ribosomal subunits in eukaryotes requires eIF5B. *Nature* **403:** 332–335

Polekhina G, Thirup S, Kjeldgaard M, Nissen P, Lippmann C, Nyborg J (1996) Helix unwinding in the effector region of elongation factor EF-Tu-GDP. *Structure* **4:** 1141–1151

Roll-Mecak A, Alone P, Cao C, Dever TE, Burley SK (2004) X-ray structure of translation initiation factor eIF2γ: implications for tRNA and eIF2γ binding. *J Biol Chem* **279:** 10634–10642

Roll-Mecak A, Cao C, Dever TE, Burley SK (2000) X-ray structures of the universal translation initiation factor IF2/eIF5B: conformational changes on GDP and GTP binding. *Cell* **103:** 781–792

Rother M, Mathes I, Lottspeich F, Böck A (2003) Inactivation of the *selB* gene in *Methanococcus maripaludis*: effect on synthesis of selenoproteins and their sulfur-containing homologs. *J Bacteriol* **185:** 107–114

Rother M, Resch A, Gardner WL, Whitman WB, Böck A (2001) Heterologous expression of archaeal selenoprotein genes directed by the SECIS element located in the 3′ non-translated region. *Mol Microbiol* **40:** 900–908

Rother M, Wilting R, Commans S, Böck A (2000) Identification and characterisation of the selenocysteine-specific translation factor SelB from the archaeon *Methanococcus jannaschii*. *J Mol Biol* **299:** 351–358

Schmitt E, Blanquet S, Mechulam Y (2002) The large subunit of initiation factor aIF2 is a close structural homologue of elongation factors. *EMBO J* **21:** 1821–1832

Selmer M, Su XD (2002) Crystal structure of an mRNA-binding fragment of *Moorella thermoacetica* elongation factor SelB. *EMBO J* **21:** 4145–4153

Shin BS, Maag D, Roll-Mecak A, Arefin MS, Burley SK, Lorsch JR, Dever TE (2002) Uncoupling of initiation factor eIF5B/IF2 GTPase and translational activities by mutations that lower ribosome affinity. *Cell* **111:** 1015–1025

Thompson JD, Gibson TJ, Plewniak F, Jeanmougin F, Higgins DG (1997) The CLUSTAL_X windows interface: flexible strategies for multiple sequence alignment aided by quality analysis tools. *Nucleic Acids Res* **25:** 4876–4882

Tujebajeva RM, Copeland PR, Xu XM, Carlson BA, Harney JW, Driscoll DM, Hatfield DL, Berry MJ (2000) Decoding apparatus for eukaryotic selenocysteine insertion. *EMBO Rep* **1:** 158–163

Valle M, Zavialov A, Li W, Stagg SM, Sengupta J, Nielsen RC, Nissen P, Harvey SC, Ehrenberg M, Frank J (2003) Incorporation of aminoacyl-tRNA into the ribosome as seen by cryo-electron microscopy. *Nat Struct Biol* **10:** 899–906

Vitagliano L, Masullo M, Sica F, Zagari A, Bocchini V (2001) The crystal structure of *Sulfolobus solfataricus* elongation factor 1α in complex with GDP reveals novel features in nucleotide binding and exchange. *EMBO J* **20:** 5305–5311

Zavacki AM, Mansell JB, Chung M, Klimovitsky B, Harney JW, Berry MJ (2003) Coupled tRNA^{Sec}-dependent assembly of the selenocysteine decoding apparatus. *Mol Cell* **11:** 773–781

Zinoni F, Heider J, Böck A (1990) Features of the formate dehydrogenase mRNA necessary for decoding of the UGA codon as selenocysteine. *Proc Natl Acad Sci USA* **87:** 4660–4664

